Nanoscale

ROYAL SOCIETY OF CHEMISTRY

MINIREVIEW

View Article Online
View Journal | View Issue

Cite this: *Nanoscale*, 2023, **15**, 6563

Labeling approaches for DNA-PAINT super-resolution imaging

Abhinav Banerjee, † Micky Anand † and Mahipal Ganji *

Super-resolution imaging is becoming a commonly employed tool to visualize biological targets in unprecedented detail. DNA-PAINT is one of the single-molecule localization microscopy-based super-resolution imaging modalities allowing the ultra-high-resolution imaging with superior multiplexing capabilities. We discuss the importance of patterned DNA nanostructures in demonstrating the capabilities of DNA-PAINT and the design of various combinations of *imager–docking strand* pairs for imaging. Central to the implementation of DNA-PAINT imaging in a biological context is the generation of *docking strand*-conjugated binders against the target molecules. Several researchers have developed a variety of labelling probes for improving resolution while also providing multiplexing capabilities for the broader application of DNA-PAINT. This review provides a comprehensive summary of the repertoire of labelling probes used for DNA-PAINT in cells and the strategies implemented to chemically modify them with a *docking strand*.

Received 22nd November 2022,
Accepted 6th March 2023

DOI: 10.1039/d2nr06541j

rsc.li/nanoscale

Introduction

In the year 1657, the father of microscopy, Antonie van Leeuwenhoek said: 'I discovered small living creatures in rainwater'. Since then, humans have never ceased peering into the microscopic realm of the living world where a plethora of molecules combine to form complex interactions and connections that humans have just begun to fathom. Super-resolution fluorescence microscopy has become an irreplaceable technique in the field of biology, enabling us to visualize structures smaller than the limits imposed on optical instruments by the phenomenon of wave diffraction, also known as the diffraction limit.[1] Super-resolution could be achieved by illuminating fluorophores in a region smaller than the diffraction limit and scanning the entire field of view, as is done in the case of Stimulated Emission Depletion microscopy (STED).[2] This method requires dedicated optical devices that can precisely control the illumination at the nanometer level. Another approach for visualizing samples beyond the diffraction limit is to regulate fluorophores to switch between fluorescence and dark mode, called blinking, thus enabling us to collect photons from individual fluorescent molecules that are separ-

Department of Biochemistry, Indian Institute of Science, Malleshwaram, Bengaluru 560012, India. E-mail: ganji@iisc.ac.in; Tel: +91 80 2293 2309
† Equal contribution.

Abhinav Banerjee

Abhinav Banerjee is a graduate student with a Prime Minister's Research Fellowship, currently pursuing his work at the Department of Biochemistry, Indian Institute of Science, Bangalore. He has completed an integrated master's degree from St. Xavier's College, Kolkata in the field of Biotechnology. He joined the Indian Institute of Science in the year 2021 and is deciphering the biophysical organizational principles of DNA and would like to extend this into developing labelling probes for super-resolution imaging.

Micky Anand

Micky Anand is a graduate student with a Prime Minister's Research Fellowship, and is currently pursuing his work at the Department of Biochemistry, Indian Institute of Science, Bangalore. He has completed his bachelor's and master's degrees from the Central University of South Bihar in the field of Life Sciences. He joined the Indian Institute of Science in the year 2021 and is interested in elucidating the role of nuclear factors in maintaining chromatin organization.

ated by distances longer than the diffraction limit. These signals can be put through Gaussian fitting algorithms to spatially localize the collected signal to sub-pixel resolution, leading to diffraction-unlimited or super-resolution imaging. This strategy, envisioned by Eric Betzig, was later termed Single Molecule Localization Microscopy (SMLM).[3] The first attempts to separate individual targets in biological specimens were to smartly regulate the on/off states of individual fluorescent protein molecules in a method called Photoactivated Localization Microscopy (PALM). In PALM, photoactivatable fluorescent proteins are stochastically switched between the on state and off state by using a low-intensity violet light.[4] Time-lapse data acquisition of blinking fluorophores allowed super-resolution microscopy when all the fitted localizations were projected simultaneously.[5,6] The novel synthesis of fluorophores that could blink with a higher quantum yield than fluorescent proteins brought in the advent of Stochastic Optical Reconstruction Microscopy (STORM). These fluorophores could be stochastically turned on and off, thus making them 'blink', enabling the fluorophore signals to be temporally separated.[7] These novel and elegant approaches for performing SMLM pushed the limits of imaging in cells but were limited mainly by (1) unavoidable fluorophore photobleaching and (2) sparsely available spectrally distinct fluorophores. Photobleaching leads to a limited photon count from each fluorophore, thus majorly compromising resolution. Sparsely available spectrally distinct fluorophores along with hardware limitations to efficiently excite and image fluorophores across a wide spectrum only allow the imaging of a few target molecular species. Due to the limited number of fluorophores bound to the samples, data can only be acquired until these molecules undergo irreversible photobleaching. Point Accumulation for Imaging in Nanoscale Topography (PAINT) was first envisioned and pursued back in 2006 where free-floating fluorophore molecules, in this case Nile Red, became immobile upon interaction with the target object, in this case a Large Unilamellar Vesicle (LUV) supported on a glass surface.[8] This technique then paved the way for circumventing the hurdle of photobleaching by using a pool of freely diffusing fluorescent molecules that only give stable fluorescence upon binding on their target molecule. DNA-PAINT super-resolution imaging takes advantage of the base-pairing interactions between two short complementary sequences.[9] It relies on transient, stochastic binding of a freely diffusing short fluorophore-labelled single-stranded DNA (ssDNA) to its complementary ssDNA immobilized on the target (Fig. 1a). One of the major breakthroughs that this technique brought about is the ability to multiplex, where a substantially higher number of targets (*i.e.*, multiplexing) could be imaged as compared with the limit imposed by spectrally distinct fluorophores. This multiplexing is possible because the target molecule identity is encoded into the DNA sequence. Many orthogonal DNA sequence pairs can easily be designed to image as many targets in a sequential manner. Nine different protein targets in the same animal cell were imaged using DNA-PAINT with unique *imager–docking strand* sequence combinations.[10] Furthermore, barcoding capabilities potentially allow the imaging of an unlimited number of targets, as shown in a study where 124 unique DNA origami targets were imaged on the same field of view in just three spectral rounds of imaging.[11] DNA-PAINT is an elegant technique that allows multiplexed quantifiable super-resolution imaging, and only necessitates a few sensitive steps for its implementation. One of the crucial strategic roadblocks is to position a *docking strand* sequence on the target of interest. This review attempts to compile the target labelling approaches, walking the reader through various methodologies utilized for both benchmarking this robust imaging tool and for imaging cellular targets.

This review is divided into four sections. The first section highlights the inseparable relationship of DNA-PAINT with DNA origami nanostructures, a programmable nano-platform used for benchmarking this technique. DNA origami nanostructures have further been used for various novel applications, where DNA-PAINT has enabled their direct observation under physiological conditions. The second section discusses various *imager–docking strand* pairs and some ingenious strategies used by researchers to further refine the DNA-PAINT imaging technique. Under section three, conjugation chemistries used to label targets in cellular samples using various immune-derived protein binders are discussed in detail. We have highlighted the role played by different heterobifunctional chemical cross-linkers in attaching *docking strands* to labelling probes. As super-resolution imaging crucially relies on the labelling probes for target flagging, we describe the currently implemented labelling strategies and their merits in detail in the fourth section. Recently, researchers have started looking for probes that reduce linkage errors by minimizing the spatial separation between the target and the *docking strand*. We highlight both conventional labelling strategies using primary and secondary antibodies with an emphasis on

Mahipal Ganji

Mahipal Ganji is a DBT-Wellcome India Alliance Intermediate Fellow and an assistant professor at the Department of Biochemistry, Indian Institute of Science, Bangalore. His lab is interested in DNA biophysics and chromatin organization. He completed his master's degree from Nizam College, Osmania University, Hyderabad, India. He went on to specialize in the field of Nanobiophysics with a master's degree from the Technical University of Dresden, Germany. He secured a Doctorate from the Technical University of Delft, The Netherlands, specializing in single-molecule biophysics. He then worked at the Max-Planck Institute of Biochemistry, Martinsried, Germany as a Marie Skłodowska-Curie postdoctoral fellow.

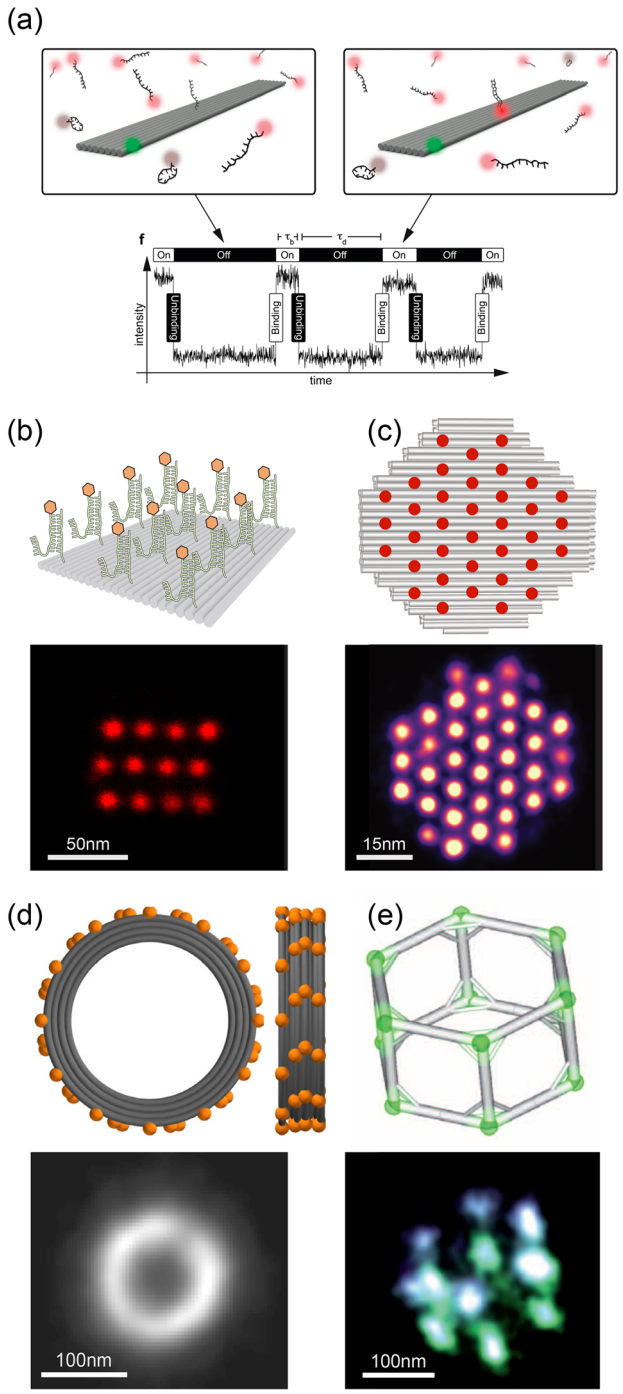

Fig. 1 Schematic representation of DNA-PAINT imaging and patterned DNA-origami nanostructures as a platform for DNA-PAINT imaging. A wide variety of shapes have been utilized for benchmarking DNA-PAINT strategies. (a) DNA-PAINT involves the transient stochastic binding of *imager strands* (carrying a red fluorophore in the figure) to the *docking strands* (immobilized) providing blinks (adapted from Jungmann *et al.*[9]). (b) A rectangular DNA origami used as a platform to display antigens to test the achievable localization precision and efficiency of the labelling probe (adapted from Ganji *et al.*[13]). (c) Hexagonal origami structures for benchmarking surface accessibility of *docking strand* on either side of the origami by *imager strands* (adapted from Eklund *et al.*[20]). (d) Cylindrical DNA origami structures used for the benchmarking of fluorogenic DNA-PAINT (adapted from Chung *et al.*[79]). (e) Polyhedral DNA origami structure imaged with 3D DNA-PAINT (adapted from Iinuma *et al.*[29]).

the linkage error they impart, and newer strategies where the use of nanobodies with a considerably smaller footprint substantially minimizes linkage errors. Lastly, we shine light on peptide-based PAINT approaches having similar working principles as DNA-PAINT along with other labelling strategies that require gene editing for engineering sites where *docking strands* can later be introduced.

DNA origami, a programmable benchmarking platform for DNA-PAINT

SMLM-based approaches for super-resolution imaging require repetitive fluorescent blinks from individual target molecules. DNA-PAINT achieves this essential 'blinking' *via* transient interactions between an *imager strand* and a target carrying a complementary *docking strand*.[9,12] While introducing *docking strands* on biological targets is tedious and limited by the labelling techniques used to visualize these targets, biological heterogeneity prohibits researchers from testing the kinetics of *imager–docking strand* pairs, achievable resolution, and labelling efficiencies under controlled settings.[13] Hence, an *in vitro* platform that enables positioning of individual *docking strands* at specified distances with high accuracy would be an ideal setup to benchmark DNA-PAINT. DNA being the most amenable biomolecule, easiest to synthesize, and its inherent nature to hybridize with its complementary sequence, *i.e.*, being programmable, makes it the ideal candidate for such an *in vitro* system. These traits allow unlimited possibilities in the design and creation of simple one-dimensional structures to complex three-dimensional multimeric nanostructures.[14,15] A long ssDNA scaffold that is generally the M13-phage genome and synthetic short ssDNA staple strands – each are complementary to two or more distant regions on the scaffold – could be self-assembled into predefined DNA origami nanostructures mainly dictated by the Franklin–Watson–Crick base pairing.[14,15]

The DNA origami structures can be designed into any imaginable shapes (Fig. 1b–e) which could be verified under an atomic force microscope (AFM) or an electron microscope (EM) with sub-nanometer accuracy. These structures carry necessary characteristics of an *in vitro* system as a nanoscopic ruler for benchmarking fluorescence-based super-resolution imaging techniques. Fluorophore-labelled staple strands positioned at defined distances within the DNA origami structures were imaged with super-resolution techniques such as direct Stochastic Optical Reconstruction Microscopy (*d*STORM) and Single-molecule High-Resolution Imaging with Photo-bleaching (SHRImP).[16–18] This was further extended for DNA-PAINT by positioning staple strands extended with *docking strands* at specified positions within the DNA origami.[9]

The staple strands used in DNA origami structures for DNA-PAINT imaging are placed at locations that ensure that they extend perpendicular to the plane of a two-dimensional

origami to make them accessible. The first DNA-PAINT imaging was done on long DNA origami structures that were either monomeric or ribbon-like multimers.[9] With further development in design and versatility, more complex structures were used to perform and benchmark the resolving ability of DNA-PAINT both in two and three dimensions. A derivative of the Rothemund rectangle evolved into a versatile tool where one could place *docking strands* at a range of distances in any possible design to be able to obtain a super-resolved image (Fig. 1b).[12,15] In fact, a graphical user interface tool, named 'Picasso-design', has been developed for efficiently designing the *docking strand* extension patterns on these rectangular nanostructures.[12] For other complex analysis of DNA-PAINT's ability, octagonal or cylindrical DNA origami structures were used (Fig. 1c and d).[19,20]

Unlike other super-resolution techniques based on sub-pixel image localization that rely on stochastic switching of fluorophores (*e.g.*, STORM or PALM), DNA-PAINT solely relies on the transient interactions of *imager–docking strand* pairs. Determining the kinetics of such transient interactions is crucial to decide the imaging parameters such as imager concentration, ionic strength of the buffer, and duration and rate of image acquisition. DNA origami structures provide a great platform for introducing a programmable number of targets with defined spatial separation and pattern. This allows measurement of the kinetics of imager binding in more controlled settings, paving the way for rationale design and characterization of imager probes to enhance the speed of imaging.[9,19,21–23]

A variant of DNA-PAINT, called quantitative-PAINT (qPAINT), can be used for estimating the number of target proteins in a given region upon *in situ* imaging.[24] The kinetics of DNA-PAINT imaging is independent of the photokinetics of the fluorophore and solely rely on the freely diffusing *imager strands*. This allows the estimation of the number of targets based on the binding kinetics of imager given that there exists a calibration in the same imaging field. DNA origami structures designed with a defined number of *docking strands* serve as an internal calibration standard. These DNA origami structures can be either microinjected into cells or fixed onto the cell surface for normalization.[24]

DNA origami structures with patterned antigens can be used for measuring the achievable resolution of DNA-PAINT. In general, labelling of targets within cells relies on using immune-derived proteins, such as antibodies or nanobodies, within fixed cells. These labels come in a wide range of sizes (from 3 to 12 nm), introducing linkage errors between the target position and the read-out signal. This becomes crucial when performing super-resolution imaging as some structures are just irresolvable due to these linkage errors introduced by large labelling probes.[25] DNA origami structures allow the measurement of the resolving limits using various labelling probes. This is made possible by attaching specific antigens to the staple sequence strand and incorporating them at fixed distances from each other within the origami structures. Imaging these antigens flagged with various labelling probes allows the measurement of the resolution limit harbored by the corresponding probes.[13]

With the evolving uses of DNA origami structures in other biological applications, DNA-PAINT has emerged as a potent tool for their direct visualization in other areas of life sciences. Biomimetic DNA origami structures carrying antigens spaced with varying distances have been used to stimulate T-cells with nanoscale precision.[26] DNA-PAINT allows ground truth visualization of the presence of antigens and their true spacing on the origami nanostructures. Complex 3D origami structures are now being used for mimicking viral structures and for therapeutic purposes.[27,28] The ability to direct visualization of DNA nanostructures under physiological conditions makes DNA-PAINT a powerful tool for structural characterization of these complex 3D structures (Fig. 1e).[21,29]

Imager–docking strand pairs

The *docking strand* and its cognate *imager strand* pair dictate the rate of binding (*on rate*) and unbinding (*off rate*). This necessitates the need for careful design of efficient oligonucleotide sequences. Ideally, these sequences need to harbor faster kinetics, such as fast *on rates* enabling the use of lower imager concentrations to reduce background noise, and *off rates* in the range that provides four to five frames of binding time for good signal-to-noise ratio.

Classical imaging strands

Initial DNA-PAINT imager probes were designed to be of nine or ten nucleotides in length.[9] These were named P-sequences, composed of all four nucleotides, and were screened exclusively based on the binding kinetics (Table 1). They showed rate constants in the range of 0.2 s^{-1} to 1.6 s^{-1} depending on the length of the imager. These sequences were used to initially tune the buffer conditions under varying imaging temperatures for DNA-PAINT super-resolution microscopy, to minimize background by reducing imager concentrations and maximizing the number of binding events for better sampling. The lower *off rate* constants were attributed to the fact that these sequences were long, thus forming a more stable DNA duplex upon binding, and lower *on rate* constants due to their tendency to form transient secondary structures. As a result, the imaging speeds with the classical imaging probes are on the order of several hours.[30] This called for designing more efficient imaging strands for image acquisition within practical time scales of a few minutes.

Imaging strands with repetitive sequences

The speed of DNA-PAINT imaging is chiefly dictated by the time interval between two binding events at the same *docking strand*. There are a range of factors that determine the binding kinetics of an *imager–docking strand* pair, including tendencies to form transient secondary structures in either of the partners. Achieving more realistic super-resolution imaging durations without compromising data sampling as compared with

Table 1 Table highlighting the various imager sequences and their cognate *docking strands*. Each bar on the 5× sequences indicates a possible docking site for imager binding. Sequences are obtained from Schnitzbauer *et al.*,[12] Schueder *et al.*,[22] Strauss and Jungmann[23] and Chung *et al.*[19]

	Imager	Sequence	Docking strand
Classical imaging strands	P1	CTAGATGTAT	TTATACATCTA
	P2	TATGTAGATC	TTATCTACATA
	P3	GTAATGAAGA	TTTCTTCATTA
	P4	GTAGATTCAT	TTATGAATCTA
	P5	CATACATTGA	TTTCAATGTAT
	P6	CTTTACCTAA	TTTTAGGTAAA
	P7	GTACTCAATT	TTAATTGAGTA
	P8	CCATTAACAT	TTATGTTAATG
	P9	CATCCTAATT	TTAATTAGGAT
	P10	GATCCATTAT	TTATAATGGAT
Repetitive imaging strands	PS3	TCCTCCC	GGGAGGA
	R1	AGGAGGA	1× TCCTCCT
			5× TCCTCCTCCTCCTCCTCCT
	R2	TGGTGGT	1× ACCACCA
			5× ACCACCACCACCACCACCA
	R3	GAGAGAG	1× CTCTCTC
			5× CTCTCTCTCTCTCTC
	R4	TGTGTGT	1× ACACACA
			5× ACACACACACACACA
	R5	GAAGAAG	1× CTTCTTC
			5× CTTCTTCTTCTTCTTCTTC
	R6	TTGTTGTT	1× AACAACAA
			5× AACAACAACAACAACAACAA
Fluorogenic paint probe A		AGAAGTAATGTGGAA	TTTCAACATATCCTCTA
Fluorogenic paint probe B		AAGAAGTAAAGGGA	CCTCGCTGAACCCCTTA

the use of classical strands required the rational design of sequences that would show much faster binding rates. The first such sequences were envisioned based on a study that compared the kinetics of seven different sequences each of eight bases in length.[31] This study laid the groundwork for the first speed sequence called PS3 for rapid imaging (Table 1), designed based on the fastest sequence.[22] This imager combined with optimal buffer conditions resulted in an order of magnitude enhancement in the imaging speed as compared with the classical P-imager sequence series. This faster binding imager was used in low concentrations for achieving similar sampling rates resulting in enhanced resolution of cellular targets. Using this speed-optimized imager, microtubule networks in human cells, which are spread over a 4×4 mm^2 area, were imaged by stitching 144 individual tiles acquired in 8 hours.

Following up on the speed-optimized sequence pair, Strauss and Jungmann extended the repertoire by six more speed sequences, named R-sequences (Table 1), that contain repeating units of either a di- or tri-nucleotide sequence.[23] By concatenating repeat units, several overlapping binding sites could be achieved without drastically increasing the length of the *docking strand*. The increase in the speed was due to the absence of secondary structures within the *docking strand*. Binding kinetics of *imager strand* on 1×, 3×, 5× and 10× repeating unit *docking strands* were studied, showing a linear correlation between the number of repeats and the binding frequency. Overall, these smartly designed sequences showed an increase in image acquisition rate by up to 100-fold as compared with the classical imager probes.

In another study, classical imager probes (*i.e.*, P-sequences) were concatenated to kinetically barcode targets to allow simultaneous multiplexed imaging.[11] The concatenated docking sites led to reduction in background noise and non-specific signals as compared with non-repeat strands.[32] The downside of the concatenated P-sequences is that the *docking strand* length increases proportionately and can form secondary structures, leading to considerably slower imaging speeds than the speed-optimized imaging probes.

Background-free imager probes

DNA-PAINT is plagued by high background noise as compared with other super-resolution techniques because the sample is immersed in a buffer containing freely diffusing *imager strands*. This sea of imagers is constantly excited by the incoming light, thus causing high background noise. This noise is significantly reduced by using Total Internal Reflection Fluorescence (TIRF) illumination that generates an evanescent field penetrating only a couple of hundred nanometers above the coverslip, thus limiting the excitation volume.

Other elegant ways to mitigate the background noise include utilizing smartly designed imaging strands that minimize the fluorescence signal when the *imager strands* are present in the unbound state. DNA-FRET-PAINT and Fluorogenic-PAINT are two such novel approaches used to minimize the background noise from the sample.[19,33,34]

Förster Resonance Energy Transfer (FRET) relies on overlap in the emission spectra of a donor fluorophore with the excitation spectra of an acceptor fluorophore. This overlap drives the transfer of energy through non-radiative decay from the

donor to the acceptor in a distance-dependent manner when the donor is excited. At around 2 nm separation, only the acceptor emits photons. This physical phenomenon was exploited to obtain background-free DNA-PAINT imaging called FRET-PAINT which could be performed in two different modalities. First, the acceptor is immobilized on the target site, thus emitting signal only when the donor-imager binds to the target site. Second, freely floating donor- and acceptor-*imager strands* simultaneously bind on the tandem *docking strand* giving rise to FRET.[33,34]

In FRET-PAINT, one can use extremely high concentrations of donor and acceptor *imager strands* (up to 200 nM) as compared with conventional DNA-PAINT (up to 20 nM), to maximize the binding rates, allowing faster image acquisition with high signal-to-noise ratio. This strategy was demonstrated in cells by imaging the microtubular network using secondary antibodies that carried a *docking strand* containing the acceptor fluorophore. The DNA-FRET-PAINT uses donor fluorophores that are excited with 488 nm wavelength and an acceptor fluorophore that has an excitation maximum at around 640 nm wavelength to minimize direct excitation. However, such a FRET pair is weakly coupled because of poor spectral overlap, resulting in low photon emission from the acceptor fluorophore and hence providing lower resolution data.

An elegant design of self-quenching *imager strands* was to incorporate a fluorophore (Cy3B or ATTO643) and its cognate spectral quencher (BHQ2 or Iowa Black FQ) at either end.[19] These *imager strands* remain dark when in solution due to their collapsed state which brings the fluorophore and the quencher in close proximity leading to fluorescence quenching (Table 1). However, in its bound state, the fluorophore is spatially separated from the quencher, allowing the fluorescence emission. Although an 8–9 nm distance provides complete de-quenching, a satisfactory signal could be obtained by a spacing of 5–6 nm between the fluorophore and the quencher. This can be achieved by separating the pair by 15 bases or more along a dsDNA. However, a 15-base complementarity between the imager and the *docking strand* would lead to stable binding (on the order of hours), thus making it incompatible with PAINT. This drawback was elegantly mitigated by introducing internal mismatches between the imager and *docking strand* pairs to destabilize the binding, driving faster *off rate* constants required for DNA-PAINT. These probes were designed to avoid any self-complementarity that could reduce the imager *on rate*. The probes chiefly relied on the inherent flexibility of single-stranded DNA to bring the quencher in proximity to the fluorophore. A 57-fold enhancement in fluorescence was observed when the imagers were bound to their cognate *docking strands* in contrast to their fluorescence in the unbound state. This strategy of background-free imaging allowed the rapid acquisition of images at speeds up to 100 Hz with high imager concentrations, as high as 250 nM. One major limitation is the design of the 15 or longer nucleotide *imager strands* with necessary mismatches while controlling the *on* and *off rate constants* with precision and still preventing any crosstalk between the orthogonal imager pairs. This study outlines only two sequences leading to two-target imaging in a single sample, thus limiting the multiplexing capabilities.

In all living organisms, genomic DNA takes the right-handed helix conformation. Application of DNA-PAINT for DNA imaging might suffer with non-specific binding of the *imager strands* on genomic DNA. To minimize this issue, left-handed DNA *imager strands* can be used for DNA-PAINT. This strategy was utilized to minimize any background from the nucleus that is speculated to arise from the non-specific binding of the imager probe to denatured genomic DNA formed during FISH protocols.[35] Left-handed imagers and *docking strands* were implemented for probing various targets in the nucleus. This strategy relies on the fact that B-DNA *imager strands* have over 20 000 cognate binding sites within the nucleus when the genome is denatured, thus potentially increasing the background noise. L-DNA on the other hand does not bind with the denatured genomic DNA, thus reducing non-specific binding. Though this novel strategy is extremely useful in nuclear target imaging, it is less accessible as L-DNA oligos are niche products making them rather economically expensive for widespread usage.

Labelling probes for target flagging

To perform DNA-PAINT super-resolution imaging, the targets of interest must be attached with a *docking strand*. General approaches for introducing *docking strands* involve labelling the target of interest *via* immune-derived proteins such as antibodies and nanobodies, or rationally designed molecules such as affimers, aptamers *etc*. The performance of a labelling probe is described in terms of the imparted linkage error, which dictates the measurable resolution. For a given labelling probe, the linkage error is the Full Width Half Maxima (FWHM) of the Gaussian fit obtained from the overlay of individual localizations from several individual antigens. The measurable resolution is generally larger than the true target size due to this linkage error which causes a physical separation of the antigen and the *docking strand* carried by the labelling probe. Thus, the labelling probes crucially dictate the achievable resolution of SMLM, which is directly related to the size of the labelling probe. In this section we describe generally used labelling probes, their characteristics in terms of multiplexing capabilities, ease of acquisition and implementation, and the localization precision (Table 2 and Fig. 2).

Primary antibody

Due to the vast portfolio of commercially available antibodies, especially against mammalian proteins, target labelling for DNA-PAINT is often performed using antibodies. These antibodies are raised in certain animals that are well known to produce large amounts against a wide variety of antigens. The antibodies are conjugated with *docking strands via* covalent linkage. This enables high multiplexing capabilities as each

Table 2 Table outlining the various advantages and drawbacks of different labeling strategies that are commonly used in DNA-PAINT. Strategies are outlined in chronological order of usage over the years. Dash (—) represents weak ability or drawback. Number of ticks (✓) represents degree of ability harbored by the labeling strategy. Asterisk indicate the information is obtained from MD simulations. Last column outlines the source for the FWHM values listed in Fig. 2

		Ease of availability	Multiplexing capability	Need genetic manipulation	Quantifying of target	FWHM calculation
2015	LifeACT and other AFFIMERS	—	✓✓✓	NO	✓✓✓	N/A
2016	nCAA click-PAINT	—	—	YES	✓✓✓	N/A
2017	Primary and secondary antibody	✓✓✓	✓	NO	—	Ganji *et al.*, *ChemPhysChem* (2021)[13]
2017	Primary antibody	✓✓✓	✓✓✓	NO	✓✓	Früh *et al.*, *ACS Nano* (2021)[36]
2017	Primary nanobody	—	✓✓✓	NO	✓✓✓	Ganji *et al. ChemPhysChem* (2021)[13]
2018	SOMAmer	—	✓✓✓	NO	✓✓✓	Strauss *et al. Nat. Methods* (2018)[45]
2019	Primary antibody with bacterial binder	✓✓	✓	NO	✓	Schlichthaerle *et al.*, *ChemBioChem* (2019)[30]
2019	SNAP- and HALO-Tag	—	✓	YES	✓✓✓	N/A
2020	Primary antibody and secondary nanobody	—	✓✓✓	NO	✓✓✓	Ganji *et al., ChemPhysChem* (2021)[13]
2020	Peptide-PAINT	—	—	NO	✓✓✓	N/A
2021	Primary antibody and secondary fab*	✓	✓✓✓	NO	✓✓✓	Früh *et al.*, *ACS Nano* (2021)[36]

target molecule is directly labelled with a corresponding antibody with a unique *docking strand* sequence. This technique, though productive, comes with its own drawbacks. Primary antibodies are sensitive to chemical perturbations, which includes addition of heterobifunctional cross-linkers and DNA *docking strands* on its surface. These modifications often drastically reduce the binding affinity to levels that make the antibody unusable for specific labelling of the target protein. Controlled labelling of these antibodies is also extremely difficult as it involves enzymatic steps for DNA *docking strand* attachment, thus leading to specificity loss and antibody degradation.[36] Although directly conjugated primary antibodies have been used for DNA-PAINT imaging,[10] this approach is seldom used due to its unpredictable nature in terms of antibody activity. The primary antibody labelling resulted in a localization precision of 9.9 nm.[36]

Primary-secondary antibody

Secondary antibodies, being polyclonal in nature, are less susceptible to loss of affinity upon chemical modifications and are more versatile for testing any primary antibody from a given origin. With a secondary antibody conjugated with a *docking stand*, one can image any primary antibody of matching species. The secondary antibody-based labelling approach can be used for imaging fewer targets limited by the number of orthogonal species used for raising the primary antibody. For example, three different target proteins labelled with a mouse, a rabbit, and a rat primary antibody can be targeted with corresponding secondary antibodies raised in orthogonal species such as donkey. In this case, the secondary antibodies will carry covalently linked orthogonal DNA *docking strands* which can be imaged in multiple rounds of Exchange-PAINT.

This labelling approach has several merits and some disadvantages. A batch of *docking strand*-conjugated secondary antibodies can be used for imaging any target if a working primary antibody is available. The polyclonal nature of the secondary antibodies leads to an increased number of *docking strands* per target protein, enabling higher frequency imager binding and thus providing a higher signal-to-noise-ratio. The first disadvantage lies in the inability to quantify target molecule species. This is due to the undefined number of *docking strands* on a secondary antibody and the unpredictable number of secondary antibodies labelling a primary antibody. Due to this, extracting quantitative information is prone to large errors. Secondly, the achievable resolution with primary-secondary antibody labelling is rather poor. Antigen-patterned DNA nanostructures revealed that the realistically achievable resolution is limited to 40 nm.[13] This limitation is due to the large size of the antibody (~10 nm). Primary and secondary antibody together introduce a linkage error of around 20 nm in spatial localization of the target molecules. Imaging of microtubules in cells using this modality resulted in the average diameter of 57 nm as opposed to the known 22 nm diameter.[30]

Nanobody

Nanobodies are engineered binders derived from unconventional camelid antibodies. These binders differ from other mammalian classes, where they only have a pair of heavy chains solely harboring the Complementarity Determining Regions (CDRs). Nanobodies are obtained by cleaving out the constant region of the heavy chain to reduce its footprint

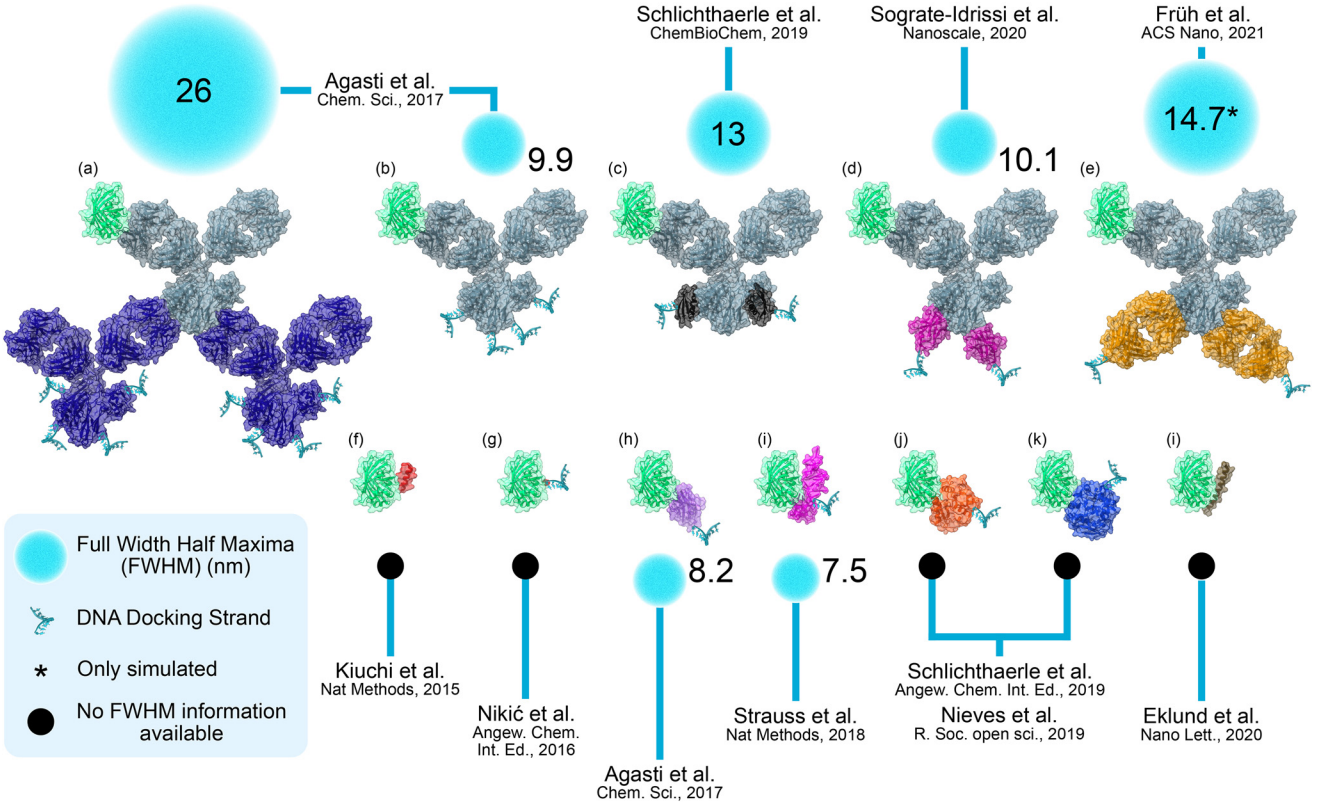

Fig. 2 Representation of the labelling probe sizes, their respective localization precision (*i.e.,* FWHM) calculated from individual antigen target and the first publication using that strategy for PAINT. For representation, these labelling probes have been shown to bind to GFP (Pdb: 3ogo). The figures have been obtained by superimposing multiple crystal structures. The cyan spheres represent the estimated spot size spread with respect to one another as described in Table 2. (a) A primary antibody (Pdb: 1igy) bound by multiple secondary antibodies (Pdb: 1igy) that carry *docking strands* labelled non-stoichiometrically. The obtained FWHM is 26 nm.[13] (b) A primary antibody carrying *docking strands*. The obtained FWHM of the localization precision is 9.9 nm.[36] (c) A primary antibody bound by bacterially derived binder protein G (Pdb: 1fcc) that carries *docking strands*. The obtained FWHM of the localization precision is 13 nm.[30] (d) A primary antibody bound by secondary nanobody (Pdb: 6xyf). The obtained FWHM of the localization precision is 10.1 nm.[13] (e) A primary antibody bound by secondary Fab fragment (Pdb: 1fdl) that carries *docking strands*. The obtained FWHM of the localization precision is 14.7 nm.[36] This value has been obtained from simulation data only and has not been performed for DNA-PAINT experimentally. (f) Direct protein binder such as Lifeact (Pdb: 7ad9) and Affirmers. (g) Protein genetically tweaked with a non-canonical Amino Acid (ncAA) to which the DNA *docking strand* is attached. (h) Primary nanobody (Pdb: 6xyf) carrying *docking strands*. The obtained FWHM of the localization precision is 8.2 nm.[13] (i) SOMAmers (Pdb: 4ni9) binding to target protein. The SOMAmer carries a DNA *docking strand* extension. The obtained FWHM of the localization precision is 7.5 nm.[45] (j) Target protein with a SNAP-tag (Pdb: 6y8p) labelled with *docking strand*. (k) Target protein with a HALO-tag (Pdb: 5uy1) labelled with *docking strand*. (l) Peptide-PAINT probe (Pdb: 1p9i) binding to the target protein directly.

during antigen labelling. Both primary and secondary nanobodies have been used extensively for DNA-PAINT. The first use of nanobodies in DNA-PAINT saw its application in imaging the mitochondrial network. Anti-Green Fluorescent Protein (GFP) nanobodies carrying the DNA *docking strand* were used for labelling mitochondrial-localized GFP.[10] This was followed by many other studies where multiple targets carrying different fluorescent proteins were visualized by their respective primary nanobodies.[37] Soon after, secondary nanobodies raised against the constant (F_c) regions of IgG antibodies obtained from different mammals were used instead of secondary antibodies. This leads to a considerable minimization of the linkage error. Furthermore, as nanobodies are expressed and produced from bacteria, they are amenable for genetic modifications. They tolerate the incorporation of additional cysteines for conjugation of *docking strands*. Because nanobodies are monoclonal in nature, only two of them bind each primary antibody. This controlled number of *docking strands* at each antigen enables accurate estimation of target molecules in each cluster. As nanobodies carry only one binding site, they can be used for labelling primary antibodies prior to their use in staining targets within the cells. This skilfully mitigates the species limitations imposed by the use of secondary antibodies, allowing multiplexing, thus truly extending the ability of DNA-PAINT to image theoretically unlimited targets within cellular structures.[38] The nanobody is much smaller in size, around 15 kDa, compared with antibodies of 150 kDa, providing comparatively better super-resolution capabilities. While primary nanobody labelling leads to around 8.2 nm of localization precision, secondary nanobody labelling resulted in 10.1 nm, showing the superiority of this approach compared with antibody-based labelling.

Bacterially obtained antibody binders protein A and protein G have also been elegantly used for DNA-PAINT. These proteins are attached with DNA *docking strands* and pre-incubated with the primary antibody to label intracellular targets. These binders have a comparable footprint to that of nanobodies, thus providing lower linkage errors.[30,39] The FWHM of the obtained localization precision for individual antigens with this labelling strategy was calculated to be 13 nm.[30]

Synthetic labeling probes

APTAMERS and SOMAmers

Aptamers are short DNA or RNA oligonucleotides that fold into specific 3D structures allowing them to specifically bind to a target molecule with high affinity.[40–42] These molecules are screened through selection procedures named Systematic Evolution of Ligands by EXponential enrichment (SELEX), where a library of short DNA or RNA oligonucleotides is incubated with the target molecule under specific conditions. The unbound oligonucleotides are separated, and the bound oligonucleotides are amplified using PCR-based techniques to enrich them. This process is repeated over 6–15 cycles with increasingly stringent conditions to ensure that only the binders with high specificity to the target molecules are retained. First introduced in 1990, this technique has been developed and modified in various ways to make the selection procedures more streamlined, minimizing any off-target bindings.[43] Slow Off-rate Modified Aptamers (SOMAmers), trademark of Somalogics Inco, were developed by incorporating chemically modified nucleotides which mimic the amino acid residues present in antibody epitopes.[41,44] DNA libraries containing a 40-nucleotide random region with 5-(*N*-benzylcarboxamide)-2′-deoxyuridine (BndU) or 5-(*N*-(1-naphthylmethyl) carboxamide)-2′-deoxyuridine (NapdU) instead of dT are used for SOMAmers screening. For DNA-PAINT, the SOMAmer sequences were extended with a *docking strand*. This allows highly specific binding to proteins of interest with high affinity and multiplexing.[45] Using this labelling approach, Strauss *et al.* achieved a FWHM of less than 8 nm when imaging EGFR, which is nearly two-fold less than that achieved when using classical primary and DNA-conjugated secondary antibodies instead. As antibodies show a multimodal distribution where a single secondary antibody carries multiple *docking strands* unlike SOMAmers, a 1 : 1 labelling of EGFR using SOMAmers could be achieved.[45] Furthermore, this approach was used to perform the first live-cell DNA-PAINT-based single-molecule tracking of EGFR on the surface of A431 cells, showing their diffusion on the lipid membrane of the cell surface.

Affimers

Affimer is a small peptide molecule derived from adhiron and human stefin A scaffold.[46] Adhiron is obtained from phytocystatin consensus sequence which inhibits cysteine proteases. Its advantage lies in its small size, monomeric nature, high stability and solubility, and lack of glycosylation sites and disulfide bonds.[47,48] The protein has the cystatin fold characterized by a four-strand anti-parallel beta sheet core and a central alpha helix.[48] Affimer developed against actin was conjugated with *docking strand* for DNA-PAINT imaging and provided an 18 nm FWHM of the actin fiber cross-section.[49]

Genetically modified tags as labelling probes

Peptide pairs as labelling reagents

Peptides were known to show transient binding to specific targets. Lifeact was one of the first peptides obtained by truncating Actin Binding Protein (Abp140) to a 17 amino acids peptide that was used to image actin filaments in cells *via* transient binding.[50] As a general approach, peptides are obtained from truncated forms of known intracellular protein binders which can be used for PAINT imaging. This transient binding between peptides and protein targets was further exploited after the discovery of more such peptide sequences that could be used to image their corresponding cellular structures. Multiple peptides derived from their partner proteins were used for super-resolution imaging in an approach called Image Reconstruction by Integrating exchangeable Single-molecule localization (IRIS).[51] Four different cellular proteins were imaged in unprecedented detail, targeting actin filaments with Lifeact, microtubules with CLIP fragment, intermediate filaments with PLEC fragment and focal adhesions with PIPKIγ fragment.[51] This technique carries an advantage over DNA-PAINT as they are direct binders and do not rely on labels such as primary and secondary antibodies for their docking, thus minimizing linkage errors and providing more accurate localization of the target over DNA-PAINT. On the flip side, such peptide binders are rare to come by and require meticulous design strategies. Glycans are saccharide complexes that are known to bind on lectin proteins present on the surface of cell. These interactions are often transient and can thus be exploited to image these cell surface lectins at super-resolution with PAINT. Glyco-PAINT utilized the transient binding of various mannose-based glycans with the mannose receptor (MR).[52] As an alternative strategy, rationally designed peptide pairs with weak binding strength were proposed for super-resolution imaging. These peptides were designed to form α-helical coils which in turn would coil around one another to form a coiled-coil interaction that is transient in nature. The Glutamate/Lysine (E/K) coiled-coil peptide pair has been widely studied and was taken up as a good candidate for super-resolution imaging purposes. The lengths of coiled-coil peptides were tuned to display transient interactions for PAINT-like imaging applications termed Peptide-PAINT.[53] The origami platforms were used for demonstrating working principles and the resolving power of Peptide-PAINT. Cellular imaging was implemented by tagging secondary antibodies with K22 peptide sequence as *docking strand* and Cy3B-labeled

E19 peptide as the *imager strand*.[53] Though imaging was performed following labelling with primary and secondary antibodies, this paved the way for the usage of synthetically designed peptide pairs for imaging. Studies have utilized similar strategies by smartly incorporating the E22 docker in the target protein and transiently transfecting the construct to allow direct imaging of the target. Imaging was performed using a LD655-labelled K19 peptide. Super-resolved images of vimentin and Golgi bodies clearly show the ability of the technology to directly image protein targets. The study further imaged surface targets in live neuronal cells that were transfected with plasmids coding for surface receptors GluA2 and Neuroligin with the E22 peptide extended from their N-termini.[54] Similar techniques involving super-resolution imaging in yeast used endogenously expressed proteins that carried a fused docking peptide. The freely floating complementary imager peptide was fused to a fluorescent protein, mNeonGreen, which was then expressed from an inducible promoter to make the system compatible with live biological systems. Peptides pairs extracted from the TRAP4-MEEVF and SYNZIP17-SYNZIP18 interacting pairs allowed the development of Live cell Imaging using reVersible intEractions PAINT (LIVE-PAINT) for imaging in live cells.[55] Peptide-PAINT is a lucrative potential alternative for DNA-PAINT as the rational design of peptides is gaining traction of late.[56,57]

Labelling *via* genetically modified tags

Protein labelling for DNA-PAINT imaging with minute linkage errors remains as one of the challenges. Most labelling techniques rely on immune-derived labels for flagging targets within cells. Genetically modified labelling tags developed from engineered self-modifying enzymes allow highly specific *docking strand* attachment on the target protein to eliminate any potential background.

Suicidal enzyme derivatives, such as SNAP-tag[58] and HALO-tag,[59] have proved to be great tools in direct protein labelling with modified ligands. The ligands form covalent bonds with the tag that is fused to the protein of interest. SNAP-tag is derived from the human DNA-repair protein O^6-alkylguanine-DNA alkyltransferase (hAGT) that irreversibly transfers an alkyl group onto a cysteine residue from its substrate O^6-alkylguanine-DNA. This feature of the enzyme has been exploited to attach various functional molecules such as fluorescent dyes, DNA oligonucleotides, and other ligands.[60–62] The SNAP-tag was also used for live-cell imaging using *d*STORM.[63] Similarly, HALO-tag was derived from the enzyme haloalkane dehalogenase from *Rhodococcus* sp. The mutation of histidine-272 from its active site into a phenylalanine residue makes the enzyme suicidal by making it form a covalent bond with its ligand during catalysis. It was just a matter of time before these highly versatile tags were used in DNA-PAINT imaging to label proteins specifically, minimizing any linkage error and non-specific labelling.

Nuclear pore complexes (NUPs) were the first targets to be imaged with the SNAP- and HALO-tag-based strategy.[25] Due to the extremely small size of the NUP complex, conventional labelling approaches using primary and secondary antibodies are not sufficient for clearly resolving these structures.[25] Genetically engineering one of the subunits of the nuclear pore complex and labelling it with DNA *docking strands* carrying the respective ligand that irreversibly attached with the SNAP- or HALO-tag enabled greater resolution than conventional labelling to be achieved. The ligands were chemically attached to 5′-amino-modified DNA *docking strands via* NHS ester chemistry. Similar strategies were deployed to develop tagPAINT where two targets, namely HALO-tagged CD3ζ and SNAP-tagged LAT proteins in T cells, were imaged within the same cell.[64]

Other approaches for genetically tweaking the target proteins and imaging them in super-resolution have utilized the genetic code expansion (GCE) strategy.[65] The GCE approach uses an amber (TAG) suppression mutant along with a unique tRNA and the corresponding tRNA synthetase enabling the incorporation of a non-canonical Amino Acid (ncAA) in the target protein. This ncAA carries a functional group (TCO; *trans*-Cyclooct-2-en-L-Lysine) which is clicked to a 1,2,4,5-tetrazine (TZ)-modified *docking strand* which can be imaged. This imaging modality is called click-PAINT.[65] This strategy of labelling has allowed imaging of both vimentin network and nuclear pore complexes. Despite the low linkage error, the major hurdle with GCE is the very low yield of the modified proteins due to the competition between the host translation machinery and the orthogonal tRNA/aminoacyl tRNA synthetase machinery.[65]

Strategies for conjugation of *docking strands* to labelling probes

Fluorescence blinking is achieved by the transient interactions of the fluorophore-labelled *imager strand* with its complementary *docking strand*. This calls for the need for a *docking strand* on the target of interest. A wide repertoire of chemical conjugation strategies has been implemented to introduce the DNA *docking strands* on the cellular targets *via* labelling probes such as antibodies. In this section, we discuss the strategies that have been used for attaching DNA *docking strands* on proteins more in the context of DNA-PAINT. First, we discuss the non-specific chemical conjugation strategies of the labelling probes, where *docking strands* are introduced non-stoichiometrically at undictated positions. Following this we describe specific conjugation strategies which target a specific moiety for a stoichiometric *docking strand* insertion away from the binding site of the labelling probe (Table 3).

Biotin–streptavidin coupling

Initial implementations of DNA-PAINT for cellular target imaging utilized commercially available biotin-modified antibodies.[66] In this case, biotinylated *docking strands* were linked to biotinylated antibodies using streptavidin in a two-step reaction. First, the biotinylated *docking strand* was incubated with streptavidin followed by incubation of the mixture with the biotinylated antibody. The *docking strand*-attached antibodies

Table 3 Features and limitations of various chemistries utilized for linking DNA *docking strands* on labelling probes

	Non-covalent interaction	Covalent interactions			
	Biotin–avidin	NHS–amine	TCO–Tz	Maleimide–sulfhydryl	DBCO–azide
Features	One of the strongest known non-covalent interactions; highly specific	Irreversible covalent coupling which prevents dissociation. Reaction products are stable in long-term storage. Amine moieties abundantly available on proteins for clicking.	Avoids the copper-induced toxicity of CuAAC. Fastest reaction of all click chemistries. High yield of products.	Reacts specifically with reduced thiol groups on the labelling probes and can achieve 1 : 1 stoichiometric labelling by introducing a free cysteine.	Avoids the copper-induced toxicity of CuAAC. Biologically inert reactants and intermediates. Reaction occurs spontaneously at physiological pH.
Limitations	Biotin is naturally present in organisms and may lead to non-targeted interactions. Four biotin molecules can bind a single avidin, thus not allowing a 1 : 1 stoichiometric labelling. The interaction can dissociate with a short incubation at 70 °C.	Difficult to achieve 1 : 1 stoichiometric labelling when amines on proteins are targeted. It often leads to a loss in antibody specificity due to excessive conjugation at the available amines.	Does not achieve 1 : 1 stoichiometric labelling if multiple accessible amines are available as TCO–NHS clicks to amine groups first followed by clicking with Tz. Instead, TCO–maleimide could be used for site-specific labelling.	Reaction is pH sensitive. At pH >8, maleimide hydrolyses to an unreactive malic acid derivative. Thiol-modified oligos can form disulfide bridges, thus needing additional reducing and purification. Incorporating a free cysteine on an antibody is impractical.	DBCO is hydrophobic and hence needs soluble linkers such as PEG to avoid precipitation of the linker. Also, the labelling probe with multiple DBCO groups might precipitate.

were used for DNA-PAINT imaging of microtubules in human cells with an apparent width of 45–47 nm for each microtubule. Multi-target imaging of microtubules and mitochondria was performed with corresponding antibodies attached with orthogonal *docking strands* and imaged using Cy3B-and Atto655-labelled *imager strands* with no detectable crosstalk between the two pairs. Furthermore, both two-dimensional and three-dimensional (3D) Exchange-PAINT was performed for imaging beta-tubulin (microtubules), COX IV (mitochondria), TGN46 (Golgi) and PMP70 (peroxisomes) in HeLa cells.[66] The 3D imaging resulted in a cross-sectional distance of ~109 nm in the *z*-axis for microtubules. This demonstrated that Exchange-PAINT is a transformative tool which allows the imaging of a substantially higher number of targets in contrast to other fluorescence-based imaging modalities which are limited by the availability of spectrally distinct fluorophores.

Covalent coupling

Covalent coupling enables the introduction of DNA *docking strands* to the labelling probes in an irreversible manner. This prevents any potential dissociation of the *docking strand* from the probe and allows the long-term storage of the labelling probes. DNA molecules can be attached *via* chemical cross-linking strategies such as *N*-hydroxysuccinimide (NHS)–Amine,[67] *trans*-cyclooctyne (TCO)–1,2,4,5-Tetrazine (Tz),[68,69] Maleimide–Sulfhydryl,[70] and Dibenzoazacyclooctyne (DBCO)–Azide Cu-free 'click' chemistry.[71] These chemistries have been exploited to develop heterobifunctional cross-linkers that carry two different reactive functional groups on the termini of a long organic spacer molecule (often Polyethylene Glycol, PEG). These heterobifunctional spacers have been used as an intermediate step in introducing the DNA *docking strand* on the labelling probes.

Amine–NHS conjugation

This chemistry is one of the most widely used conjugation strategies, thanks to its compatibility with a wide range of conditions, widespread availability of amine moieties on protein labelling probes, and high specificity and efficiency. The NHS–ester moiety is often used to attach bifunctional cross-linkers, non-specifically to accessible primary amines present on a protein (Fig. 3a and b). An amide bond is formed between the primary amine and carbonyl of the ester group during the reaction with NHS as the leaving group. This strategy has its own drawbacks, which include a loss in antibody specificity due to modifications in the paratope of the antibody and lack of control over the number of cross-linkers bound.[37] This results in a non-uniform number of *docking strands* conjugated to each antibody (sometimes none) and accumulation of hydrophobic functional groups (DBCO) around it affecting its solubility.[72] Additionally, proximity of the *docking strand* to the antibody will also interfere with its accessibility to the *imager strands*. To circumvent this, spacers like Poly(Ethylene Glycol) $(PEG)_n$ have been introduced to increase the solubility of the protein and the accessibility of the *docking strands* to the *imager strands*.[72,73] Amine-based linkers are also used for site-specific tagging of antibodies, discussed in greater detail below (Fig. 3c).[36]

Thiol–maleimide conjugation

DNA strands with the thiol group on one of their termini are commercially synthesized. These DNA molecules can be conjugated to a heterobifunctional cross-linker carrying a maleimide group. Maleimide forms a thio-ester bond with the thiol group, which is relatively stable at physiological conditions.[74] The availability of free thiol groups on protein surfaces in the reduced form is rare, due to the oxidizing physiological conditions. This is exploited by designing labelling probes carry-

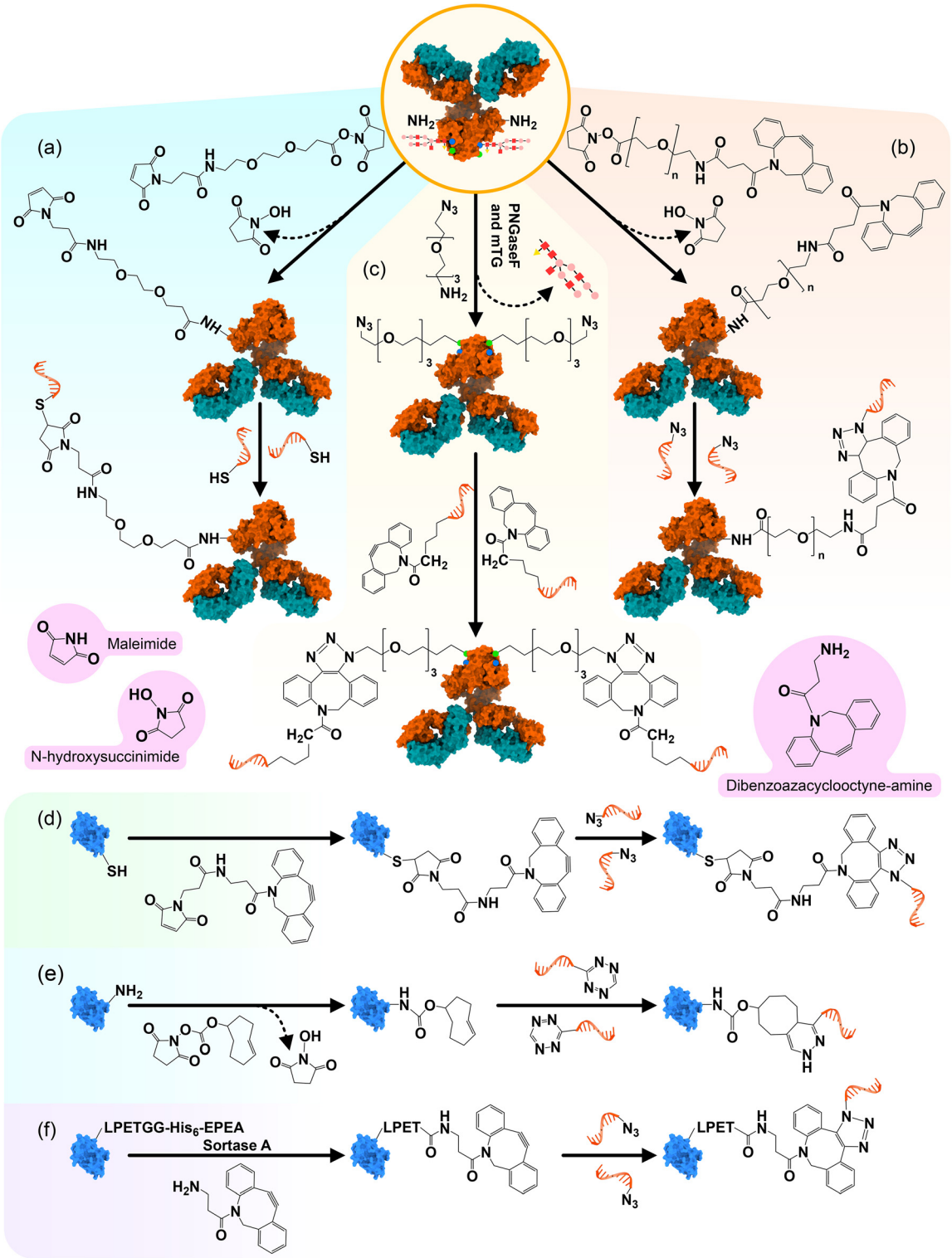

Fig. 3 Schematic representation showing various heterobifunctional cross-linkers used for conjugating DNA *docking strands* to DNA-PAINT labelling probes. (a) Maleimide–$(PEG)_n$–NHS ester cross-linker; (b) DBCO–$(PEG)_n$–NHS ester cross-linker; (c) deglycosylation followed by mTG-mediated transfer of azide carrying cross-linker; (d) DBCO–maleimide cross-linker; (e) TCO–TZ cross-linker; and (f) sortase A-mediated transfer of DBCO carrying cross-linker. Antibody (Pdb: 1igy); Nanobody (Pdb: 6xyf).

ing a single cysteine residue, thus preventing disulfide formation, and making the thiol group available for the reaction in a site-specific manner, discussed later in greater detail. However, this approach comes with its own drawbacks. At alkaline pH (pH ≥8), maleimide can undergo hydrolysis forming an unreactive malic acid amide derivative, thus calling for careful preparation of buffer and pH maintenance.[75] Another drawback of this method is the formation of disulfide bridges between the thiol-modified oligos requiring additional disulfide reducing and purification steps.

TCO–Tz conjugation

Another approach to form covalent bonds within biomolecules is to use the TCO (*trans*-cyclooctene)–Tz (1,2,4,5-tetrazine) conjugation strategy where amine-functionalized DNA *docking strands* are clicked to Tz–NHS ester cross-linker, which enables the addition of a Tz functional group on the DNA. On the other hand, the labelling probe is incubated with TCO–NHS ester, thus adding a free TCO functional group on lysine residues on the surface of the label. These two constituents are then pooled together, thus enabling the TCO on the probe to react with the Tz-containing *docking strand* mediated by the strain-promoted inverse-electron-demand Diels–Alder cycloadditions (SPIEDAC) reaction.[68,69]

Azide–DBCO conjugation

Another alternative approach widely utilized for covalently linking DNA strands with labelling probes is to utilize the strain-promoted alkyne–azide cycloadditions (SPAAC) copper-free click chemistry.[71] The DNA *docking strands* are obtained with an azide modification on one of the termini. Alternatively, amine-modified DNA can be conjugated with a heterobifunctional group carrying succinimidyl-ester and an azide moiety on either end. Addition of DNA *docking strands* carrying an azide is easily performed under physiological conditions. This reaction is carried out by reacting a cyclooctyne (DBCO) with azide moieties, which takes advantage of the fact that a bond angle deformation of the acetylene to 163° results in a ring strain of 18 kcal mol^{-1}.[71] This ground state destabilization accelerates the reaction towards the unstrained transition state forming products.

Uses of various heterobifunctional spacers

The first use of heterobifunctional cross-linkers to generate labelling probes for DNA-PAINT utilized the **maleimide–$(PEG)_n$–NHS** ester chemistry (Fig. 3a and d). In this scheme, the NHS ester group of the cross-linker reacts to primary amines of lysine residues on the antibody, forming a covalent bond with them. Subsequently the maleimide group reacts to the thiol-functionalized DNA *docking strands*.[24] The antibodies prepared in this manner were utilized to perform qPAINT where they calculated the number of Nup98 units in a nuclear pore complex. The conjugation protocol was further optimized to obtain ~1 *docking strand* per secondary antibody, which was confirmed using mass spectrometry.[10] The authors imaged microtubules and obtained a cross-sectional width of ~40 nm, and were thus able to visualize the hollow tubular structure of the microtubules which was not seen earlier with biotin-conjugated labelling probes. This strategy comes with the drawbacks faced by the maleimide–thiol chemistry.

Similarly, primary amines of lysine residues on primary anti-GFP nanobodies were reacted with the **TCO–NHS ester** linker. Amine-functionalized DNA *docking strands* were then reacted with **Tz–NHS ester** (Fig. 3e). The stoichiometry of this reaction was verified through mass shifts in matrix-assisted laser desorption/ionization-mass spectrometry (MALDI-MS), obtaining ~1 *docking strand* per nanobody. Mitochondria were imaged using an elegant strategy where the researchers target emGFP to the mitochondria using CellLight™ Mitochondria-GFP, BacMam 2.0, and then stain the cells using primary anti-GFP nanobodies carrying the DNA *docking strand*. TCO-TZ chemistry was also employed for linking *docking strands* to phalloidin, a bicyclic heptapeptide which selectively targets F-actin.[10] Similar chemistry was utilized for preparing bacterially derived antibody binders, Protein A or Protein G, for DNA-PAINT imaging of microtubules and EGFR in human cells.[30]

DBCO containing heterobifunctional cross-linkers was used for antibody labelling. **DBCO-sulfo-NHS** ester cross-linker was utilized for conjugating azide-functionalized DNA *docking strands* non-specifically to free amine moieties on secondary antibodies.[12,73] DBCO-NHS cross-linkers containing PEG spacers proved to be more readily soluble and were thus preferred over sulfo-containing cross-linkers.[12,73] **DBCO-$(PEG)_n$-NHS** ester cross-linkers were used for DNA-PAINT-ERS (E = Ethylene carbonate, R = Repeating sequence, and S = Spacer) where ethylene carbonate was included in the imaging buffer to speed up the off rates of the *imager strand* from the *docking strand* without affecting the reverse reaction.[73] A study emphasizing the potential drawbacks of using large protein labelling probes strategically managed to control the counts of DNA *docking strands* on a secondary antibody by using 2 : 1, 5 : 1 and 10 : 1 molar excess of azide-modified DNA *docking strands* over the linker-conjugated secondary antibodies and obtained an average of 6, 10, and 19 *docking strands* per antigen.[13]

Stoichiometric labelling strategies

The methods described above only used stoichiometric control of labelling probes and *docking strands* to achieve a certain desired number of DNA *docking strands* on the probe. These approaches, though easy to implement, always come with some degree of error as the reaction is uncontrolled. Several controlled labelling approaches for covalently linking DNA *docking strands* at a chemically unique, well-defined site to maximize the population of labelling probes carrying the desired number of DNA *docking strands* have been used.[36] Cysteines have proved to be an indispensable player in such labelling strategies.[13] Strategies to incorporate a single DNA

docking strand on nanobodies required ectopic modification with a cysteine that is exposed on the surface for chemical modification. A maleimide–DBCO cross-linker was used to obtain the desired single DNA *docking strand* per nanobody (Fig. 3d). A study used P1, P2, and P3 *imager-docking strand* combinations to obtain three-color images of mitochondria, Golgi and chromatin with a resolution of ~20 nm.[37] A similar strategy was implemented to attach one or two DNA *docking strands* to nanobodies. The anti-ALFA-tag and anti-rabbit IgG nanobodies were modified with two cysteines, one each at the N- and C-terminus. DBCO–PEG4–maleimide linker was used to click to cysteines on the nanobody for conjugating with azide-modified *docking strands* (Fig. 3d).[13]

The approach of incorporating an ectopic cysteine for controlled addition of the number of DNA *docking strands* on the labelling probe is not feasible with antibodies due to the presence of several cysteines. A more strategic approach was used, where the glycan groups that are present in all secreted IgG antibodies were specifically targeted (Fig. 3c).[36] The IgG antibodies were deglycosylated using PNGase F (peptide-*N*-glycosidase F) which is an amidase that cleaves the covalent bond between the innermost *N*-acetylglucosamine (GlcNAc) and the amino acid residue.[76] Upon removal of the N-linked glycan moieties, microbial transglutaminase enzyme was used to crosslink the amine group of the **amine–polyethylene glycol–azide** (H_2N-PEG_3-N_3) cross-linker to the amide of the glutamine at (-2) position of the deglycosylated site. The azide group of the cross-linker is then ready for clicking a DBCO–single-stranded DNA *docking strand* (Fig. 3c). The motivation behind this strategy is that there exists a glutamine residue at the (-2) position from the N-linked glycosylation site that is conserved across species and subtypes of IgG. Since each heavy chain has one such site, a maximum of two DNA *docking strands* per antibody is achievable. However, mouse IgG3 is unique as it contains two N-linked glycosylation sites on each heavy chain at N322, leading to as many as four *docking strands* per antibody.[36] This labelling strategy is not applicable to IgGs obtained from rabbits as the glutamine residue is present at the (-3) position instead of (-2), making them inaccessible to modifications. A similar restriction applies to manatees and mouse IgG2, which lack the glutamine and thus cannot be labelled by this chemistry.[36]

Nanobodies with enzymatically modifiable labelling tags were developed to enhance the DNA *docking strand* attaching efficiency. A sortase A (SrtA) recognition sequence (LPETG) was introduced at the C-terminus of the nanobody (Fig. 3f).[77] In this scheme, LPETG was extended with His_6-tag followed by EPEA allowing an engineered SrtA to cleave out GG–His_6–EPEA peptide forming a nanobody–LPET–SrtA intermediate.[77] A DBCO–amine linker substitutes SrtA, resulting in DBCO-modified nanobody. *Docking strands* with azide moiety are reacted with the DBCO–nanobody to obtain a nanobody carrying the DNA *docking strand*. With this approach, microtubules were imaged with a FWHM of 31 ± 4 nm and the plasma membrane caveolae with a diameter of 61 ± 17 nm, which is very close to the actual diameters of 25 nm and 60 nm, respectively, showing minimal linkage error.[77]

Challenges and perspectives

Super-resolution imaging using DNA-PAINT has been made possible using the low-cost inverted TIRF microscope.[78] Now the field is more focused on the design and production of more efficient labelling probes such as nanobodies, aptamers, affimers, and genetically engineered tags (including SNAP-tag, HALO-tag, and coiled-coil peptide pairs), which have a high binding affinity and allow multiplexed imaging. As the 'blinking' is achieved by the *imager strand* binding on its complementary *docking strand*, imaging durations are usually around an hour or longer depending on the kinetics of the *imager strand* sequences. Recent development of speed-optimized imager sequences (R-sequences) using di- and tri-nucleotide repeats in combination with optimized buffer conditions dramatically improved image acquisition rates by up to a 100-fold.[22,23] However, the latter are limited to six *imager–docking strand* pairs, thus dictating imaging of that many targets only. This highlights the need to design a larger repertoire of speed-optimized probes for enhanced multiplexing capabilities which could unlock the potential of DNA-PAINT. *Imager strands* tend to show non-specific off-target binding that could lead to imaging artifacts. Continuous efforts are being directed to mitigate this limitation, for example by developing fluorogenic-PAINT, FRET-PAINT, and left-handed DNA-PAINT modalities.[19,33–35] The design of smarter imaging probes that could mitigate the background noise and imaging artifacts of DNA-PAINT will extend its application in multiplexed tissue-level super-resolution imaging to become an invaluable tool in biomedical diagnostics.

Conclusions

Recently, DNA-PAINT has evolved as an indispensable tool for probing biological samples at ultra-high resolution. Its implementation, however, requires amalgamation of DNA nanotechnology, chemical engineering, development of novel labelling probes that introduce minimal linkage errors, and unique orthogonal DNA *imager–docking strand pairs*. With an explosion in the number of publications discussing various approaches used for tackling each of these issues, it is tedious for researchers to efficiently exploit this technique. This review consolidates methods employed for benchmarking DNA-PAINT utilizing DNA nanostructures, all the available labelling probes used for flagging target molecules, novel click chemistries for conjugation of DNA *docking strand* on the labelling probes, and currently implemented *imager–docking strand* pairs. We also described the achievable resolution with each of the labelling probes so far implemented, along with their merits and demerits. As a whole, DNA-PAINT super-resolution imaging requires the development of more efficient imaging probes and *imager–docking strand* pairs for much wider application in biological and biomedical applications.

Glossary

Imager strand	Short DNA oligonucleotide carrying a fluorophore, is freely diffusing in the imaging solution, and complementary to *docking strand*.
Docking strand	Short DNA oligonucleotide attached to the target of interest and complementary in sequence to the *imager strand*.
Labelling probe	An organic molecule such as antibody, nanobody, aptamer, *etc*. that is carrying a DNA *docking strand* and binds to the target of interest.
Linkage error	The spatial distance introduced by a labelling probe between the true target position and the DNA *docking strand* that is imaged. This error is imparted due to the bulky nature of the labelling probe.
Exchange-PAINT	Sequential rounds of DNA-PAINT imaging. Imagers of one species are washed out of the sample to make way for another imager species that is used for imaging of the next target of interest. Multiple such rounds can be performed one after the other to image a large number of targets without spectral overlapping issues.
qPAINT	Quantitative-PAINT where the exact number of DNA *docking strand*s, and thus target concentration, can be assayed with the help of an internal normalizer, in most cases a DNA origami.
Localization precision	The spread of all the localizations from individual antigens is summed up, fit with Gaussian function, and the obtained full width at half maxima of the fit is called localization precision.
Resolution of SMLM	Localization precision calculated from nearest neighbor analysis would dictate the spread of each localized target in true space. This value gives a good approximation of the obtainable resolution that is generally 2.5 times the localization precision obtained.

Conflicts of interest

There are no conflicts to declare.

Acknowledgements

We would like to thank Dr Thomas Schlichthaerle for his valuable suggestions regarding the manuscript. The authors thank DBT-Wellcome India Alliance and the DST-SERB for funding their research. A. B. and M. A. acknowledge support from the Prime Minister's Research Fellowship (PMRF), Ministry of Education, Government of India.

References

1 K. Prakash, B. Diederich, R. Heintzmann and L. Schermelleh, Super-resolution microscopy: a brief history and new avenues, *Philos. Trans. R. Soc., A*, 2022, **380**, 20210110, DOI: **10.1098/rsta.2021.0110**.
2 T. A. Klar, S. Jakobs, M. Dyba, A. Egner and S. W. Hell, Fluorescence microscopy with diffraction resolution barrier broken by stimulated emission, *Proc. Natl. Acad. Sci. U. S. A.*, 2000, **97**, 8206–8210, DOI: **10.1073/pnas.97.15.8206**.
3 E. Betzig, Proposed method for molecular optical imaging, *Opt. Lett.*, 1995, **20**, 237–239, DOI: **10.1364/ol.20.000237**.
4 R. M. Dickson, A. B. Cubitt, R. Y. Tsien and W. E. Moerner, On/off blinking and switching behaviour of single molecules of green fluorescent protein, *Nature*, 1997, **388**, 355–358, DOI: **10.1038/41048**.
5 E. Betzig, *et al.*, Imaging intracellular fluorescent proteins at nanometer resolution, *Science*, 2006, **313**, 1642–1645, DOI: **10.1126/science.1127344**.
6 H. Shroff, H. White and E. Betzig, Photoactivated localization microscopy (PALM) of adhesion complexes, *Curr. Protoc. Cell Biol.*, 2008, DOI: **10.1002/0471143030.cb0421s41**.
7 M. J. Rust, M. Bates and X. Zhuang, Sub-diffraction-limit imaging by stochastic optical reconstruction microscopy (STORM), *Nat. Methods*, 2006, **3**, 793–796, DOI: **10.1038/nmeth929**.
8 A. SSov and R. M. Hochstrasser, Wide-field subdiffraction imaging by accumulated binding of diffusing probes, *Proc. Natl. Acad. Sci. U. S. A.*, 2006, **103**, 18911–18916, DOI: **10.1073/pnas.0609643104**.
9 R. Jungmann, *et al.*, Single-Molecule Kinetics and Super-Resolution Microscopy by Fluorescence Imaging of Transient Binding on DNA Origami, *Nano Lett.*, 2010, **10**, 4756–4761, DOI: **10.1021/nl103427w**.
10 S. S. Agasti, *et al.*, DNA-barcoded labeling probes for highly multiplexed Exchange-PAINT imaging, *Chem. Sci.*, 2017, **8**, 3080–3091, DOI: **10.1039/C6SC05420J**.
11 O. K. Wade, *et al.*, 124-Color Super-resolution Imaging by Engineering DNA-PAINT Blinking Kinetics, *Nano Lett.*, 2019, **19**, 2641–2646, DOI: **10.1021/acs.nanolett.9b00508**.
12 J. Schnitzbauer, M. T. Strauss, T. Schlichthaerle, F. Schueder and R. Jungmann, Super-resolution microscopy with DNA-PAINT, *Nat. Protoc.*, 2017, **12**, 1198–1228, DOI: **10.1038/nprot.2017.024**.
13 M. Ganji, T. Schlichthaerle, A. S. Eklund, S. Strauss and R. Jungmann, Quantitative Assessment of Labeling Probes for Super-Resolution Microscopy Using Designer DNA Nanostructures, *ChemPhysChem*, 2021, **22**, 911–914, DOI: **10.1002/cphc.202100185**.
14 F. Hong, F. Zhang, Y. Liu and H. Yan, DNA Origami: Scaffolds for Creating Higher Order Structures, *Chem. Rev.*,

2017, **117**, 12584–12640, DOI: **10.1021/acs.chemrev.6b00825**.

15 P. W. K. Rothemund, Folding DNA to create nanoscale shapes and patterns, *Nature*, 2006, **440**, 297–302, DOI: **10.1038/nature04586**.

16 C. Steinhauer, R. Jungmann, T. L. Sobey, F. C. Simmel and P. Tinnefeld, DNA Origami as a Nanoscopic Ruler for Super-Resolution Microscopy, *Angew. Chem., Int. Ed.*, 2009, **48**, 8870–8873, DOI: **10.1002/anie.200903308**.

17 M. Heilemann, *et al.*, Subdiffraction-Resolution Fluorescence Imaging with Conventional Fluorescent Probes, *Angew. Chem., Int. Ed.*, 2008, **47**, 6172–6176, DOI: **10.1002/anie.200802376**.

18 M. P. Gordon, T. Ha and P. R. Selvin, Single-molecule high-resolution imaging with photobleaching, *Proc. Natl. Acad. Sci. U. S. A.*, 2004, **101**, 6462–6465, DOI: **10.1073/pnas.0401638101**.

19 K. K. H. Chung, *et al.*, Fluorogenic DNA-PAINT for faster, low-background super-resolution imaging, *Nat. Methods*, 2022, **19**, 554–559, DOI: **10.1038/s41592-022-01464-9**.

20 A. S. Eklund, A. Comberlato, I. A. Parish, R. Jungmann and M. M. C. Bastings, Quantification of Strand Accessibility in Biostable DNA Origami with Single-Staple Resolution, *ACS Nano*, 2021, **15**, 17668–17677, DOI: **10.1021/acsnano.1c05540**.

21 S. F. J. Wickham, *et al.*, Complex multicomponent patterns rendered on a 3D DNA-barrel pegboard, *Nat. Commun.*, 2020, **11**, 5768, DOI: **10.1038/s41467-020-18910-x**.

22 F. Schueder, *et al.*, An order of magnitude faster DNA-PAINT imaging by optimized sequence design and buffer conditions, *Nat. Methods*, 2019, **16**, 1101–1104, DOI: **10.1038/s41592-019-0584-7**.

23 S. Strauss and R. Jungmann, Up to 100-fold speed-up and multiplexing in optimized DNA-PAINT, *Nat. Methods*, 2020, **17**, 789–791, DOI: **10.1038/s41592-020-0869-x**.

24 R. Jungmann, *et al.*, Quantitative super-resolution imaging with qPAINT, *Nat. Methods*, 2016, **13**, 439–442, DOI: **10.1038/nmeth.3804**.

25 T. Schlichthaerle, *et al.*, Direct Visualization of Single Nuclear Pore Complex Proteins Using Genetically-Encoded Probes for DNA-PAINT, *Angew. Chem., Int. Ed.*, 2019, **58**, 13004–13008, DOI: **10.1002/anie.201905685**.

26 J. Hellmeier, *et al.*, DNA origami demonstrate the unique stimulatory power of single pMHCs as T cell antigens, *Proc. Natl. Acad. Sci. U. S. A.*, 2021, **118**, e2016857118, DOI: **10.1073/pnas.2016857118**.

27 J. R. Burns, B. Lamarre, A. L. B. Pyne, J. E. Noble and M. G. Ryadnov, DNA Origami Inside-Out Viruses, *ACS Synth. Biol.*, 2018, **7**, 767–773, DOI: **10.1021/acssynbio.7b00278**.

28 C. Sigl, *et al.*, Programmable icosahedral shell system for virus trapping, *Nat. Mater.*, 2021, **20**, 1281–1289, DOI: **10.1038/s41563-021-01020-4**.

29 R. Iinuma, *et al.*, Polyhedra Self-Assembled from DNA Tripods and Characterized with 3D DNA-PAINT, *Science*, 2014, **344**, 65–69, DOI: **10.1126/science.1250944**.

30 T. Schlichthaerle, M. Ganji, A. Auer, O. K. Wade and R. Jungmann, Bacterially Derived Antibody Binders as Small Adapters for DNA-PAINT Microscopy, *ChemBioChem*, 2019, **20**, 1032–1038, DOI: **10.1002/cbic.201800743**.

31 M. Schickinger, M. Zacharias and H. Dietz, Tethered multi-fluorophore motion reveals equilibrium transition kinetics of single DNA double helices, *Proc. Natl. Acad. Sci. U. S. A.*, 2018, **115**, E7512–E7521, DOI: **10.1073/pnas.1800585115**.

32 A. H. Clowsley, *et al.*, Repeat DNA-PAINT suppresses background and non-specific signals in optical nanoscopy, *Nat. Commun.*, 2021, **12**, 501, DOI: **10.1038/s41467-020-20686-z**.

33 A. Auer, M. T. Strauss, T. Schlichthaerle and R. Jungmann, Fast, Background-Free DNA-PAINT Imaging Using FRET-Based Probes, *Nano Lett.*, 2017, **17**, 6428–6434, DOI: **10.1021/acs.nanolett.7b03425**.

34 J. Lee, S. Park and S. Hohng, Accelerated FRET-PAINT microscopy, *Mol. Brain*, 2018, **11**, 70, DOI: **10.1186/s13041-018-0414-3**.

35 H. J. Geertsema, *et al.*, Left-handed DNA-PAINT for improved super-resolution imaging in the nucleus, *Nat. Biotechnol.*, 2021, **39**, 551–554, DOI: **10.1038/s41587-020-00753-y**.

36 S. M. Früh, *et al.*, Site-Specifically-Labeled Antibodies for Super-Resolution Microscopy Reveal In Situ Linkage Errors, *ACS Nano*, 2021, **15**, 12161–12170, DOI: **10.1021/acsnano.1c03677**.

37 S. Sograte-Idrissi, *et al.*, Nanobody Detection of Standard Fluorescent Proteins Enables Multi-Target DNA-PAINT with High Resolution and Minimal Displacement Errors, *Cells*, 2019, **8**, 48, DOI: **10.3390/cells8010048**.

38 S. Sograte-Idrissi, *et al.*, Circumvention of common labelling artefacts using secondary nanobodies, *Nanoscale*, 2020, **12**, 10226–10239, DOI: **10.1039/D0NR00227E**.

39 G. A. O. Cremers, B. J. H. M. Rosier, R.R. Brillas, L. Albertazzi and T. F. A. de Greef, Efficient Small-Scale Conjugation of DNA to Primary Antibodies for Multiplexed Cellular Targeting, *Bioconjugate Chem.*, 2019, **30**, 2384–2392, DOI: **10.1021/acs.bioconjchem.9b00490**.

40 A. D. Ellington and J. W. Szostak, In vitro selection of RNA molecules that bind specific ligands, *Nature*, 1990, **346**, 818–822, DOI: **10.1038/346818a0**.

41 L. Gold, *et al.*, Aptamer-Based Multiplexed Proteomic Technology for Biomarker Discovery, *PLoS One*, 2010, **5**, e15004, DOI: **10.1371/journal.pone.0015004**.

42 C. Tuerk and L. Gold, Systematic Evolution of Ligands by Exponential Enrichment: RNA Ligands to Bacteriophage T4 DNA Polymerase, *Science*, 1990, **249**, 505–510, DOI: **10.1126/science.2200121**.

43 H. Y. Kong and J. Byun, Nucleic Acid aptamers: new methods for selection, stabilization, and application in biomedical science, *Biomol. Ther.*, 2013, **21**, 423–434, DOI: **10.4062/biomolther.2013.085**.

44 S. Kraemer, *et al.*, From SOMAmer-Based Biomarker Discovery to Diagnostic and Clinical Applications: A SOMAmer-Based, Streamlined Multiplex Proteomic Assay, *PLoS One*, 2011, **6**, e26332, DOI: **10.1371/journal.pone.0026332**.

45 S. Strauss, *et al.*, Modified aptamers enable quantitative sub-10 nm cellular DNA-PAINT imaging, *Nat. Methods*, 2018, **15**, 685–688, DOI: **10.1038/s41592-018-0105-0**.
46 C. Tiede, *et al.*, Affimer proteins are versatile and renewable affinity reagents, *eLife*, 2017, **6**, e24903, DOI: **10.7554/eLife.24903**.
47 L. K. Stadler, *et al.*, Structure-function studies of an engineered scaffold protein derived from Stefin A. II: Development and applications of the SQT variant, *Protein Eng., Des. Sel.*, 2011, **24**, 751–763, DOI: **10.1093/protein/gzr019**.
48 C. Tiede, *et al.*, Adhiron: a stable and versatile peptide display scaffold for molecular recognition applications, *Protein Eng., Des. Sel.*, 2014, **27**, 145–155, DOI: **10.1093/protein/gzu007**.
49 T. Schlichthaerle, *et al.*, Site-Specific Labeling of Affimers for DNA-PAINT Microscopy, *Angew. Chem., Int. Ed.*, 2018, **57**, 11060–11063, DOI: **10.1002/anie.201804020**.
50 J. Riedl, *et al.*, Lifeact: a versatile marker to visualize F-actin, *Nat. Methods*, 2008, **5**, 605–607, DOI: **10.1038/nmeth.1220**.
51 T. Kiuchi, M. Higuchi, A. Takamura, M. Maruoka and N. Watanabe, Multitarget super-resolution microscopy with high-density labeling by exchangeable probes, *Nat. Methods*, 2015, **12**, 743–746, DOI: **10.1038/nmeth.3466**.
52 R. Riera, *et al.*, Single-molecule imaging of glycan–lectin interactions on cells with Glyco-PAINT, *Nat. Chem. Biol.*, 2021, **17**, 1281–1288, DOI: **10.1038/s41589-021-00896-2**.
53 A. S. Eklund, M. Ganji, G. Gavins, O. Seitz and R. Jungmann, Peptide-PAINT Super-Resolution Imaging Using Transient Coiled Coil Interactions, *Nano Lett.*, 2020, **20**, 6732–6737, DOI: **10.1021/acs.nanolett.0c02620**.
54 B. K. Maity, D. Nall, Y. Lee and P. R. Selvin, Peptide-PAINT Using a Transfected-Docker Enables Live- and Fixed-Cell Super-Resolution Imaging, *Small Methods*, 2023, 2201181, DOI: **10.1002/smtd.202201181**.
55 C. Oi, *et al.*, LIVE-PAINT allows super-resolution microscopy inside living cells using reversible peptide-protein interactions, *Commun. Biol.*, 2020, **3**, 458, DOI: **10.1038/s42003-020-01188-6**.
56 A. M. Webster and A. F. Peacock, De novo designed coiled coils as scaffolds for lanthanides, including novel imaging agents with a twist, *Chem. Commun.*, 2021, **57**, 6851–6862, DOI: **10.1039/D1CC02013G**.
57 Y. Yano and K. Matsuzaki, Live-cell imaging of membrane proteins by a coiled-coil labeling method—Principles and applications, *Biochim. Biophys. Acta, Biomembr.*, 2019, **1861**, 1011–1017, DOI: **10.1016/j.bbamem.2019.02.009**.
58 A. Keppler, *et al.*, A general method for the covalent labeling of fusion proteins with small molecules in vivo, *Nat. Biotechnol.*, 2003, **21**, 86–89, DOI: **10.1038/nbt765**.
59 G. V. Los, *et al.*, HaloTag: A Novel Protein Labeling Technology for Cell Imaging and Protein Analysis, *ACS Chem. Biol.*, 2008, **3**, 373–382, DOI: **10.1021/cb800025k**.
60 D. Maurel, *et al.*, Cell-surface protein-protein interaction analysis with time-resolved FRET and snap-tag technologies: application to GPCR oligomerization, *Nat. Methods*, 2008, **5**, 561–567, DOI: **10.1038/nmeth.1213**.
61 G. J. Gu, *et al.*, Protein tag-mediated conjugation of oligonucleotides to recombinant affinity binders for proximity ligation, *New Biotechnol.*, 2013, **30**, 144–152, DOI: **10.1016/j.nbt.2012.05.005**.
62 A. Gautier, E. Nakata, G. Lukinavičius, K.-T. Tan and K. Johnsson, Selective Cross-Linking of Interacting Proteins Using Self-Labeling Tags, *J. Am. Chem. Soc.*, 2009, **131**, 17954–17962, DOI: **10.1021/ja907818q**.
63 T. Klein, *et al.*, Live-cell dSTORM with SNAP-tag fusion proteins, *Nat. Methods*, 2011, **8**, 7–9, DOI: **10.1038/nmeth0111-7b**.
64 D. J. Nieves, *et al.*, tagPAINT: covalent labelling of genetically encoded protein tags for DNA-PAINT imaging, *R. Soc. Open Sci.*, 2023, **6**(12), 191268, DOI: **10.1098/rsos.191268**.
65 I. Nikić, *et al.*, Debugging Eukaryotic Genetic Code Expansion for Site-Specific Click-PAINT Super-Resolution Microscopy, *Angew. Chem., Int. Ed.*, 2016, **55**, 16172–16176, DOI: **10.1002/anie.201608284**.
66 R. Jungmann, *et al.*, Multiplexed 3D cellular super-resolution imaging with DNA-PAINT and Exchange-PAINT, *Nat. Methods*, 2014, **11**, 313–318, DOI: **10.1038/nmeth.2835**.
67 G. W. Anderson, J. E. Zimmerman and F. M. Callahan, N-hydroxysuccinimide esters in peptide synthesis, *J. Am. Chem. Soc.*, 1963, **85**, 3039–3039, DOI: **10.1021/ja00902a047**.
68 M. L. Blackman, M. Royzen and J. M. Fox, Tetrazine ligation: fast bioconjugation based on inverse-electron-demand Diels– Alder reactivity, *J. Am. Chem. Soc.*, 2008, **130**, 13518–13519, DOI: **10.1021/ja8053805**.
69 N. K. Devaraj, R. Weissleder and S. A. Hilderbrand, Tetrazine-based cycloadditions: application to pretargeted live cell imaging, *Bioconjugate Chem.*, 2008, **19**, 2297–2299, DOI: **10.1021/bc8004446**.
70 C. Lee and E. Samuels, Adducts from the reaction of N-ethylmaleimide with l-cysteine and with Glutathione, *Can. J. Chem.*, 1961, **39**, 1152–1154, DOI: **10.1139/v61-143**.
71 N. J. Agard, J. A. Prescher and C. R. Bertozzi, A Strain-Promoted [3 + 2] Azide–Alkyne Cycloaddition for Covalent Modification of Biomolecules in Living Systems, *J. Am. Chem. Soc.*, 2004, **126**, 15046–15047, DOI: **10.1021/ja044996f**.
72 J. Wiener, D. Kokotek, S. Rosowski, H. Lickert and M. Meier, Preparation of single- and double-oligonucleotide antibody conjugates and their application for protein analytics, *Sci. Rep.*, 2020, **10**, 1457, DOI: **10.1038/s41598-020-58238-6**.
73 F. Civitci, *et al.*, Fast and multiplexed superresolution imaging with DNA-PAINT-ERS, *Nat. Commun.*, 2020, **11**, 1–8, DOI: **10.1038/s41467-020-18181-6**.
74 T. Miyadera and E. M. Kosower, Receptor site labeling through functional groups. 2. Reactivity of maleimide groups, *J. Med. Chem.*, 1972, **15**, 534–537, DOI: **10.1021/jm00275a024**.
75 L. Martínez-Jothar, *et al.*, Insights into maleimide-thiol conjugation chemistry: Conditions for efficient surface

functionalization of nanoparticles for receptor targeting, *J. Controlled Release*, 2018, **282**, 101–109, DOI: **10.1016/j.jconrel.2018.03.002**.

76 D. A. Fischler and R. Orlando, N-linked Glycan Release Efficiency: A Quantitative Comparison between NaOCl and PNGase F Release Protocols, *J. Biomol. Tech.*, 2019, **30**, 58–63, DOI: **10.7171/jbt.19-3004-001**.

77 V. Fabricius, J. Lefebre, H. Geertsema, S. F. Marino and H. Ewers, Rapid and efficient C-terminal labeling of nanobodies for DNA-PAINT, *J. Phys. D: Appl. Phys.*, 2018, **51**(47), 474005, DOI: **10.1088/1361-6463/aae0e2**.

78 A. Auer, *et al.*, Nanometer-scale Multiplexed Super-Resolution Imaging with an Economic 3D-DNA-PAINT Microscope, *ChemPhysChem*, 2018, **19**, 3024–3034, DOI: **10.1002/cphc.201800630**.

79 K. K. H. Chung, *et al.*, Fluorogenic probe for fast 3D whole-cell DNA-PAINT, *bioRxiv*, 2020.2004.2029.066886, 2020. DOI: **10.1101/2020.04.29.066886**.